SUPPLEMENTAL MATERIAL

Fig1- SM: ***Comparison of the catalytic modules of LytC and other members of the GH25 family.***

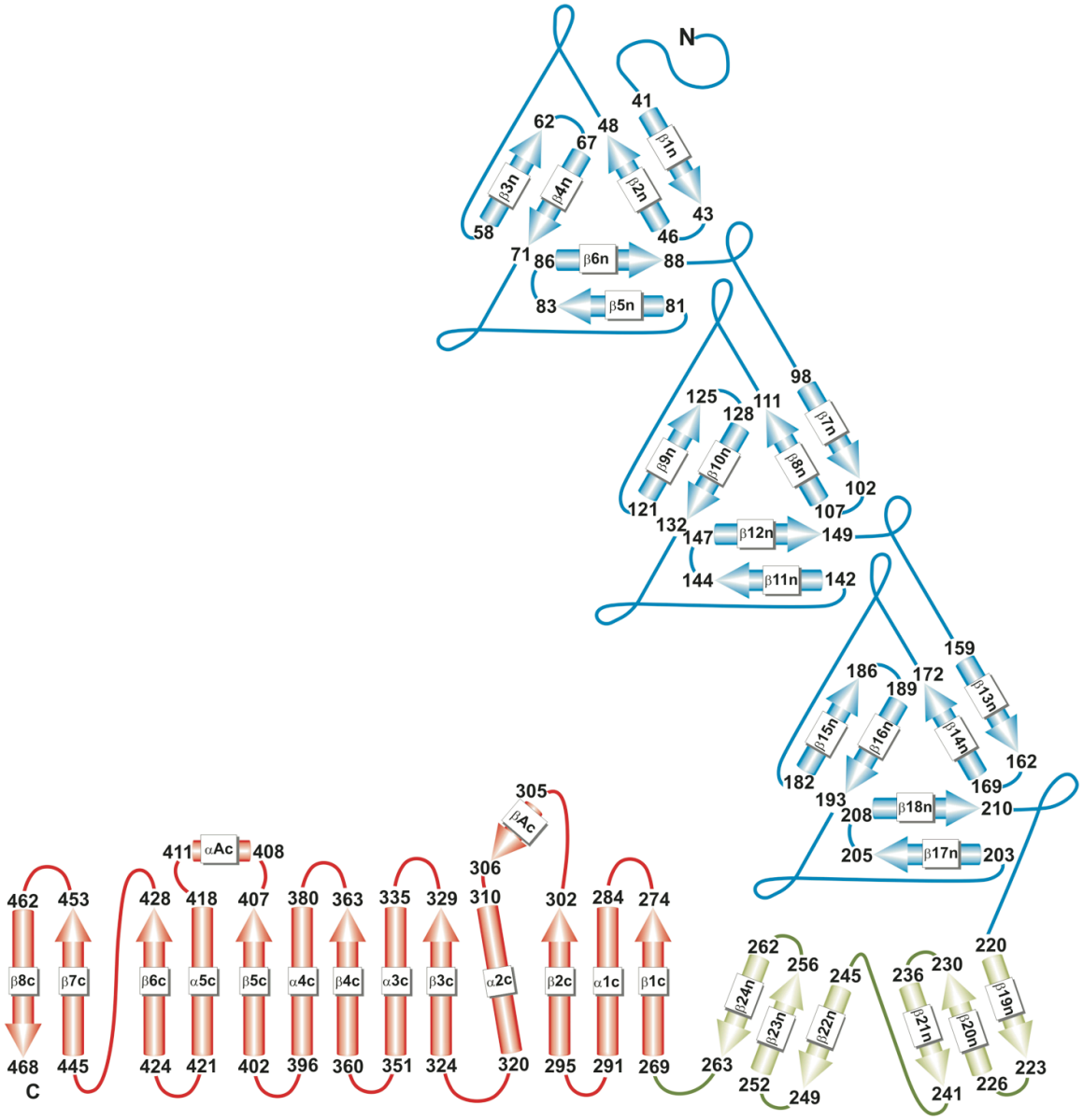

Figure 1a

Figure 1b

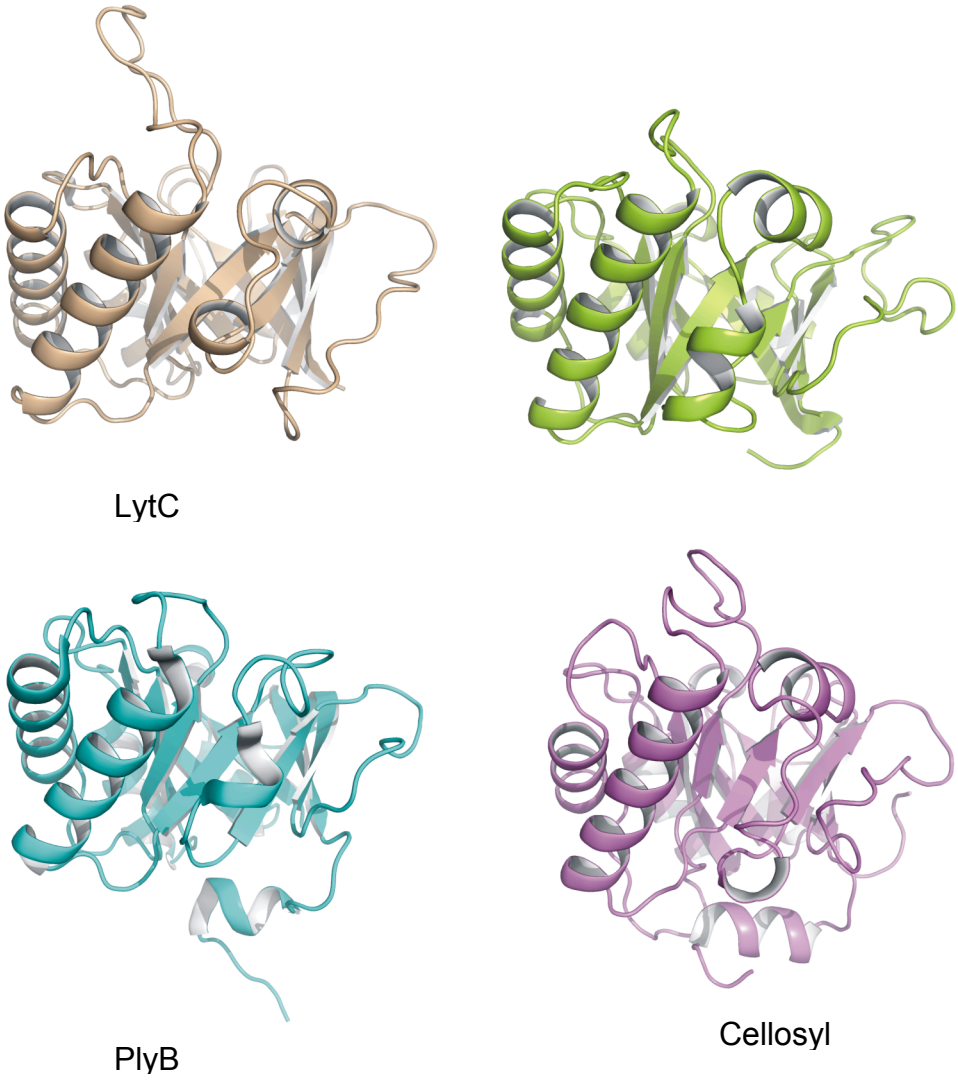

Figure 1c: Superimposition of CM_{LytC} (beige), CM_{Cpl-1} (green), Cellosyl (violet) and PlyB (cyan)

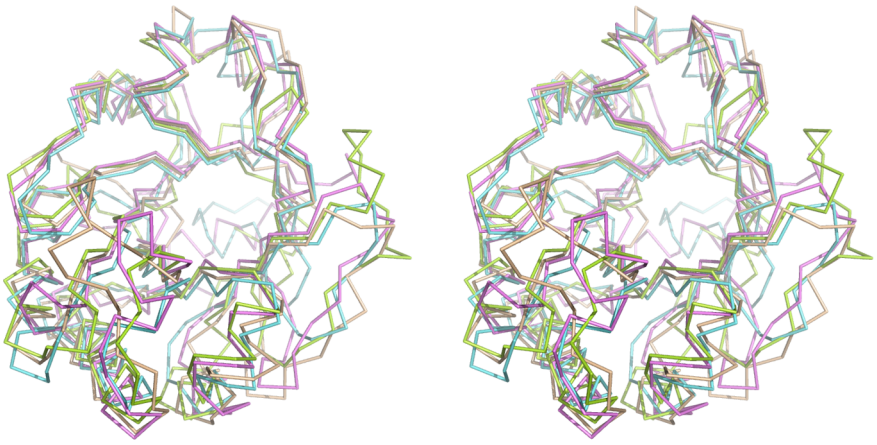

Comparison of the catalytic module of LytC with other members of the GH25 family. Structural superimposition of the catalytic module of LytC (CM_{LytC}) with the structures of the glycosyl hydrolases of the GH25 family reported until now: Cpl-1 (ref1-SM), Cellosyl (ref2-SM) and PlyB (ref3-SM), shows that the core of the CM_{LytC} structure is conserved with respect to the other members of the GH25 family (Figure1-SM), as reflected by the low rmsd values summarized in Table 1-SM. Significant differences in the overall structure locate in the following α-helices and loops flanking the central β-barrel: the α1c (residues 284-291), the N-t of the α3c and α3c-β4c loop (residues 348-359), the β4c-α4c loop (residues 364-379), the helices αAc and α5c (residues 408-421), the loop β6c-β7c (residues 429-444), the loop β7c-β8c (residues 454-461), and the C-terminal of β8c. Most of these regions are found near the interface between the catalytic module and the cell-wall anchoring module in both LytC and Cpl-1 (Figure3-SM). The β4c-α4c loop (Lc loop) adjacent to the active site, displays significant differences in extension and composition in the case of LytC with respect the other GH25 members. In LytC, this loop is 11-aa longer than in PlyB, 8-aa longer than in Cpl-1 endolysin, and 2-aa longer than in Cellosyl. Sequence alignment of LytC with other members of the GH25 family reveals that Lc is unique among the GH25 family.

Table1-SM: Rmsd values obtained from the superimposition of the CM of LytC with other structures of the GH25 family.

GH	Cpl-1 (CM)	Cellosyl	PlyB
Rmsd (Å)	1.86	1.52	1.60
No. Cα atoms	144	167	156

Fig2-SM: Intermodular interactions in LytC

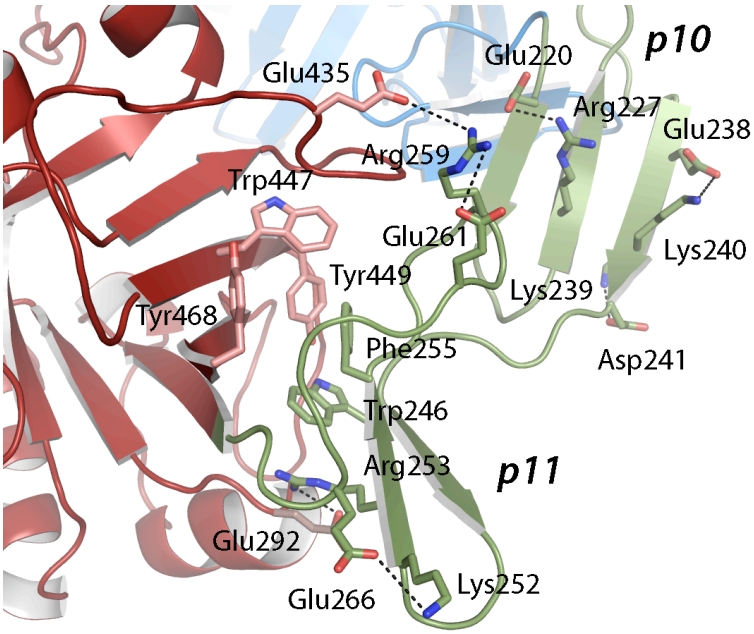

Intermodular interactions in LytC. LytC structure is formed by an N-terminal choline-binding module, and by a C-terminal catalytic module. The interface between both modules is built by amino acids belonging to the *p*11 repeat of the CBM and to the CM. The interface is stabilized by hydrophobic and salt-bridge contacts which are represented in Figure 2-SM.

Fig3-SM: Teichoic acid binding at GYMA sites

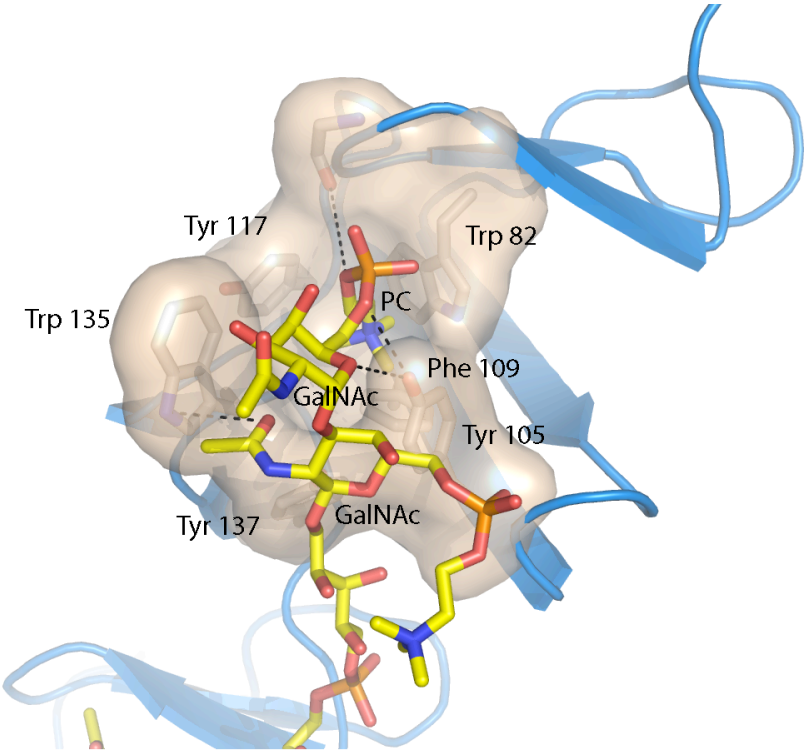

Docked model of the teichoic acid into the GYMA sites as obtained by GOLD (ref). Residues building the GYMA site and the teichoic acid moieties bound are labelled. Dashed lines indicate predicted polar interactions.

Fig4-SM:

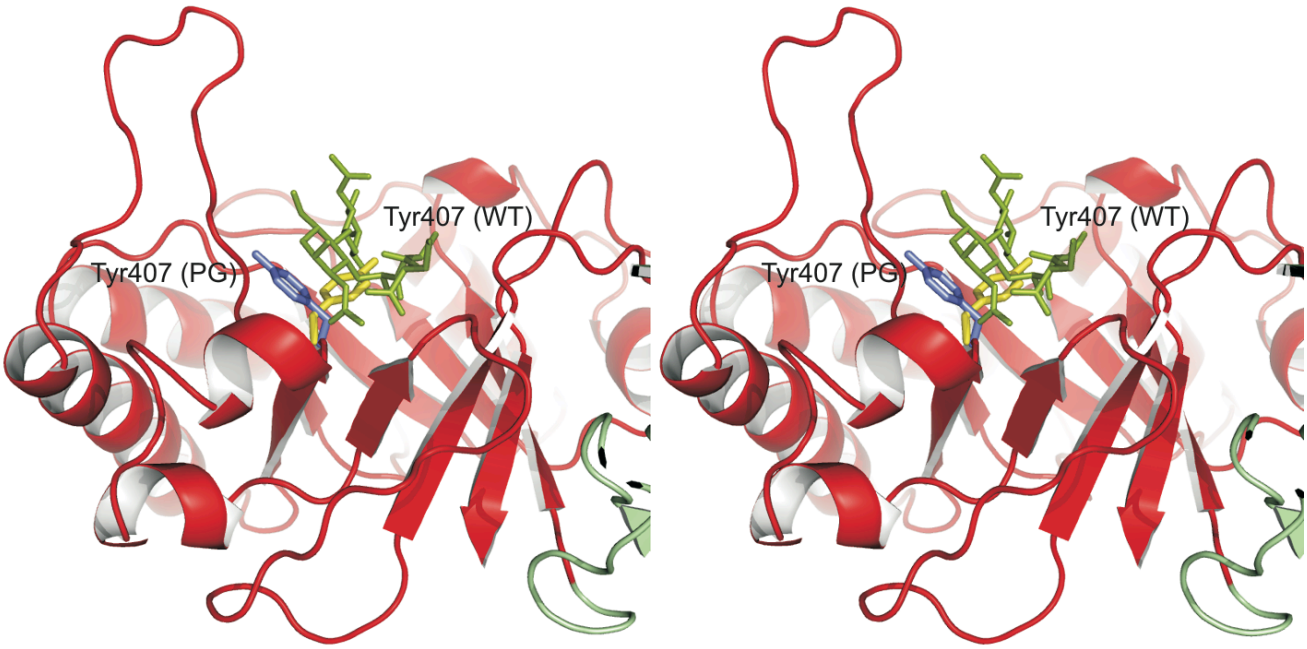

Access mechanism to the active site of LytC by the substrate. In the absence of substrate Tyr407 blocks the entrance to the active site (*A)*; upon ligand binding, Tyr407 repositions itself to allow access to the substrate and interacts with it to stabilize its binding *(B)*.

Fig5-SM:

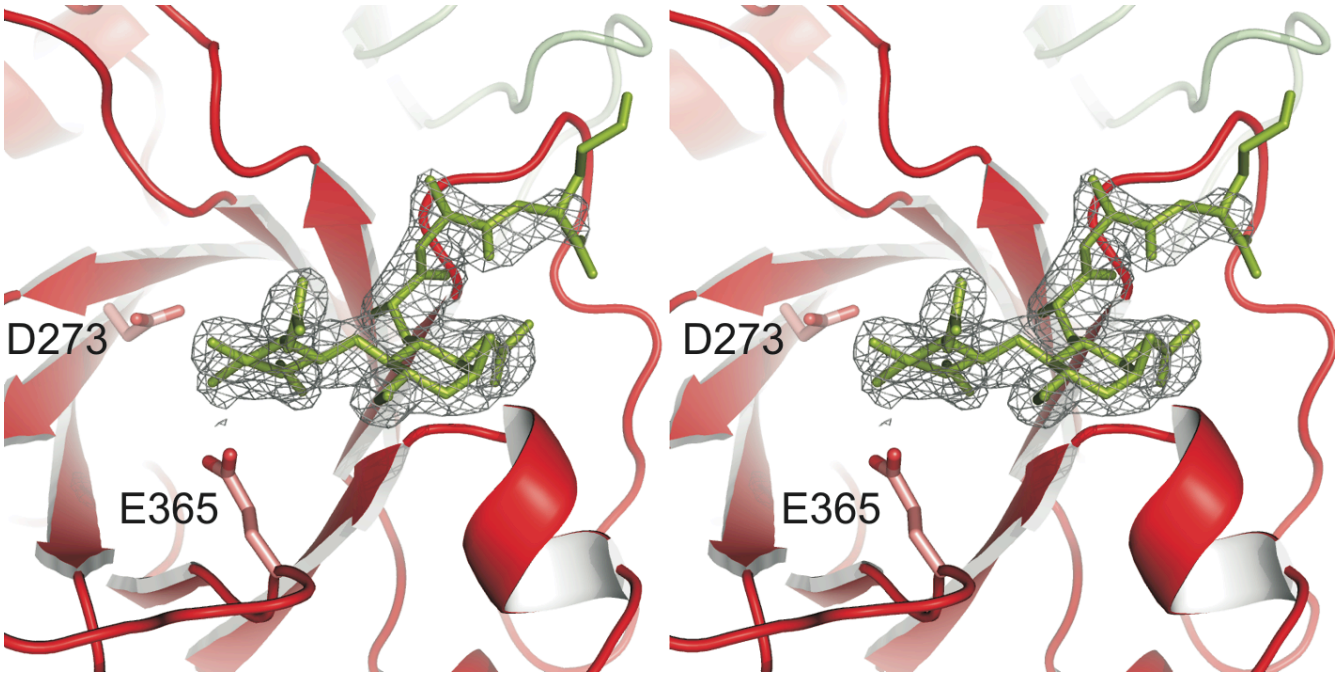

Electron density map observed for the pneumococcal PG fragment of the crystallographic complex. Stereoview representation of the complex. Electron density map ($2F_o$-F_c) is contoured at 1.0 σ in grey. Carbon atoms of the ligand are in green and the protein is in red.

Fig6-SM: Peptidoglycan-binding sites in LytC and Cpl-1

(A)

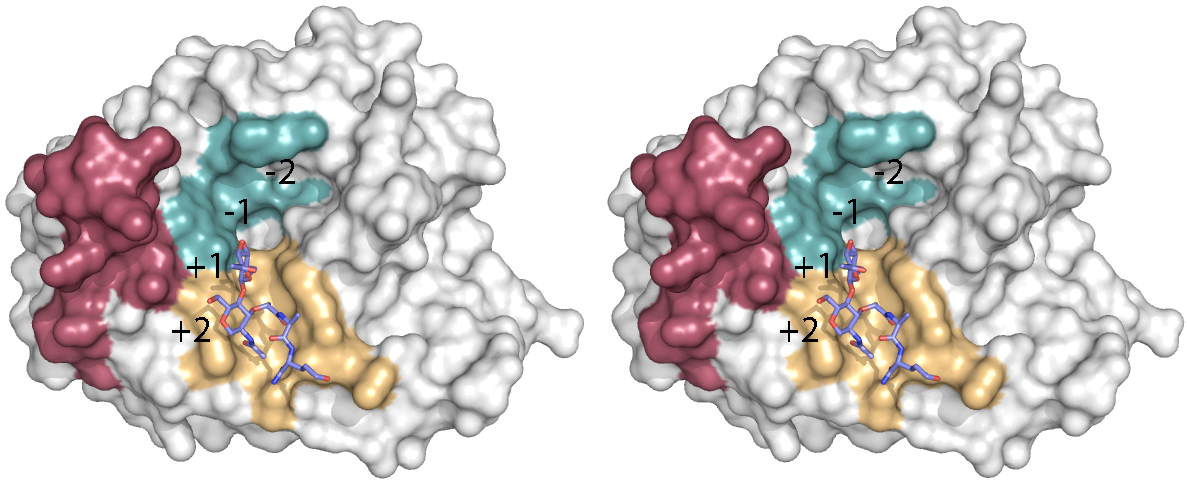

(B)

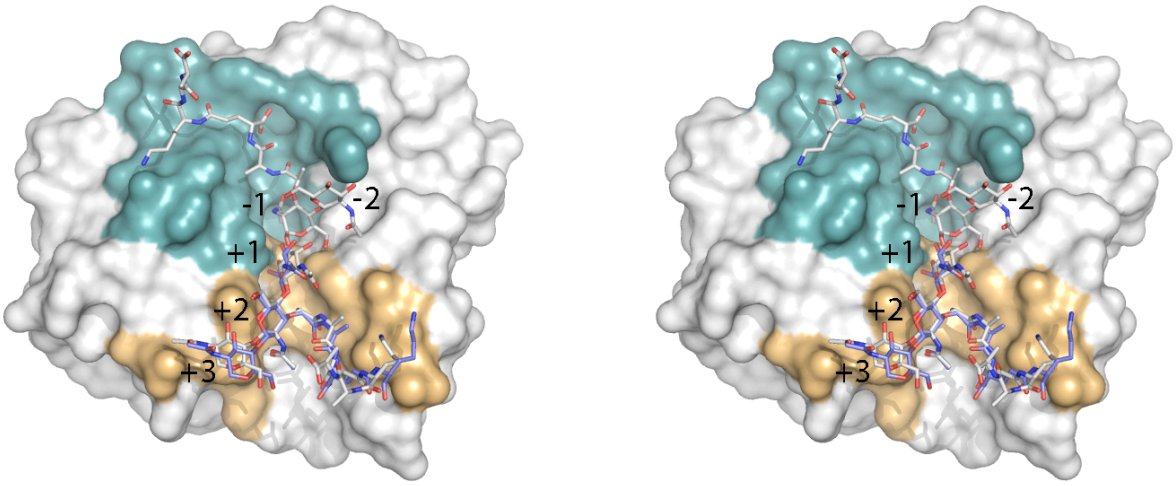

Figure legend: (A) Stereoview of the molecular surface of LytC in complex with a pneumococcal PG fragment. PG-binding sites +1 and +2 are highlighted in orange while sites -1 and -2 are coloured in blue. Positions of the substrate rings are labelled. Lc loop is coloured in dark red. (B) Stereoview of the molecular surface of Cpl-1 in complex with $(2S5P)_2$ (blue sticks) superimposed with the docked model for $(2S5P)_3$ substrate (white sticks) (ref). PG-binding sites +1/+2 and -1/-2 are highlighted as in (A).

Peptidoglycan-binding sites in LytC

Further analysis of the CM of LytC shows complete conservation of the active centre of LytC with respect to Cpl-1, Cellosyl and PlyB structures (see Figure4A-SM). The two catalytic residues (D273 and E365) are structurally observed as well as the distance between them, which agrees with the hydrolytic mechanism with inversion of the configuration proposed for this family of hydrolases (ref1-SM). Analysis of the PG-binding channel clearly shows a full conservation of the PGBS1 of LytC with respect to Cpl-1 (see Table2-SM. LytC also presents the mobile tyrosine found in Cpl-1 (Y407 in LytC and Y127 in Cpl-1) which, in both hydrolases, suffers the same rearrangement upon PG binding making accessible the PG-binding channel (ref4-SM). On the contrary, PGBS2 displays remarkable differences with respect to Cpl-1, Cellosyl and PlyB in: 1) the Lc loop is markedly longer in LytC and does not display sequence homology with respect to other GH of the family, 2) the molecular surface and amino-acid composition in the groove stabilizing the peptide stem at position -1 (Figure3-SM). LytC lacks the salt-bridge network found in the PGBS2 of Cpl-1, Cellosyl and PlyB, which was proposed to stabilize the peptide stem of the PG (in -1) (ref4-SM). In LytC, a hydrophobic channel built by three

tyrosines and one valine (Y302, Y331, Y369 and V370) is found instead of this salt-bridge network.

Table2-SM: Correspondence of amino-acids of the PG-binding site in LytC and other GH25 members (Inma, aqui no se ven las diferencias en el Lc loop de LytC frente a las demas; quizas tambien habria que dividir los aminoacidos de cada PGBS en glycan chain recognition and peptide stem recognition).

Header				
	LytC	**Cpl-1 (CM)**	**Cellosyl**	**PlyB**
PGBS1	E365	E94	E100	E92
	Y405	Y125	Y138	Y121
	Y407	Y127	T140	H124
	R408	K128	A141	_
	S409	P129	S142	H125
	A428	A151	A163	P143
	_	_	H164	_
	Y430	Y153	W165	Y145
PGBS2	D10	D273	D9	D6
	S12	S275	S11	S8
	S13	E276	H12	K9
	H14	H277	W13	W10
	K34	R299	K33	R29
	E37	Y302	E36	D32
	Y41	K305	Y40	Y36
	Y59	Y327	Y62	Y58
	F61	Y329	F64	F60
	R63	Y331	R66	R62
	D92	D363	D98	D90
	E94	E365	E100	E92
	_	Y369	_	_
	D182	D467	D198	D171
Notes.				

References

Ref1-SM. Monterroso, B., Albert, A., Galán, B., Ahrazem, O., García, P., Martínez-Ripoll, M., García, J.L. & Menéndez, M. Structural basis for selective recognition of pneumococcal cell wall by modular endolysin from phage Cp-1. *Structure* **11**, 1239-1249 (2003).

Ref2-SM. Rau, A., Hogg, T., Marquardt, R. & Heilgenfeld, R. A new lysozyme fold. Crystal structure of the muramidase from *Streptomyces coloelicolor* at 1.65 A resolution. *J. Biol. Chem*. **276**, 31994-31999 (2001).

Ref3-SM. Porter, C. J., Schuch, R., Pelzek, A. J., Buckle, A. M., McGowan, S., Wilce, M. C., Rossjohn, J., Russell, R., Nelson, D., Fischetti, V. A. & Whisstock, J. C. The 1.6 A crystal structure of the catalytic domain of PlyB, a bacteriophage lysin active against *Bacillus anthracis*. *J. Mol. Biol.* **366**, 540-550 (2007).

Ref4-SM. Pérez-Dorado, I. Campillo, N. E., Monterroso,B., Hesek, D., Lee, M., Páez, J. A., García, P., Martínez-Ripoll, M., García, J. L., Mobashery, S., Menéndez, M. & Hermoso, J. A. Elucidation of the molecular recognition of bacterial cell wall by modular pneumococcal phage endolysin CPL-1. *J. Biol. Chem.* **282**, 24990-24999 (2007)